ELSEVIER

Brain & Development 36 (2014) 10–15

BRAIN & DEVELOPMENT
Official Journal of the Japanese Society of Child Neurology

www.elsevier.com/locate/braindev

Original article

Quantitative evaluation of ventricular dilatation using computed tomography in infants with congenital cytomegalovirus infection

Kiyomi Matsuo [a,1], Ichiro Morioka [a,*,1], Mai Oda [b], Yoko Kobayashi [d], Yuji Nakamachi [d], Seiji Kawano [d], Miwako Nagasaka [a], Tsubasa Koda [a], Tomoyuki Yokota [a], Satoru Morikawa [a], Akihiro Miwa [a], Akio Shibata [a], Toshio Minematsu [e], Naoki Inoue [f], Hideto Yamada [c], Kazumoto Iijima [a]

[a] *Department of Pediatrics, Kobe University Hospital, Kobe, Japan*
[b] *Department of Radiology, Kobe University Hospital, Kobe, Japan*
[c] *Department of Obstetrics and Gynecology, Kobe University Hospital, Kobe, Japan*
[d] *Department of Clinical Laboratory, Kobe University Hospital, Kobe, Japan*
[e] *Research Center for Disease Control, Aisenkai Nichinan Hospital, Nichinan, Japan*
[f] *Department of Virology I, National Institute of Infectious Disease, Tokyo, Japan*

Received 1 October 2012; received in revised form 19 December 2012; accepted 20 December 2012

Abstract

Background: Infants with congenital cytomegalovirus infection (CCMVI) may develop brain abnormalities such as ventricular dilatation, which may potentially associate with sensorineural hearing loss. There is currently no recognized method for quantitative evaluation of ventricle size in infants with CCMVI. Our objectives were to establish a method for quantitative evaluation of ventricle size using computed tomography (CT) in infants with CCMVI, and determine a cut-off value associated with abnormal auditory brainstem response (ABR) early in life.

Design/Subjects: This study enrolled 19 infants with CCMVI and 21 non-infected newborn infants as a control group. Infants with CCMVI were divided into two subgroups according to ABR at the time of initial examination: normal ABR (11 infants) or abnormal ABR (8 infants). Ventricle size was assessed by calculating Evans' index (EI) and lateral ventricle width/hemispheric width (LVW/HW) ratio on brain CT images, and was compared among groups. A cut-off ventricle size associated with abnormal ABR was determined.

Results: EI and LVW/HW ratio were significantly higher in the CCMVI with abnormal ABR group than the control and CCMVI with normal ABR groups. Cut-off values of 0.26 for EI and 0.28 for LVW/HW ratio had a sensitivity of 100% and 100%, respectively, and a specificity of 73% and 91%, respectively, for association with abnormal ABR.

Conclusions: We established a method for quantitative evaluation of ventricle size using EI and LVW/HW ratio on brain CT images in infants with CCMVI. LVW/HW ratio had a more association with abnormal ABR in the early postnatal period than EI.

Keywords: Auditory brainstem response; Cytomegalovirus infection; Evans' index; Lateral ventricle width/hemispheric width ratio; Ventricle

1. Introduction

Cytomegalovirus (CMV) is the main pathogen causing congenital infection in developed countries [1] and

* Corresponding author. Address: Department of Pediatrics, Kobe University Hospital, 7-5-1 Kusunoki-cho, Chuo-ku, Kobe 650-0017, Japan. Tel.: +81 78 382 6090; fax: +81 78 382 6099.
E-mail address: ichim@med.kobe-u.ac.jp (I. Morioka).
[1] These authors contributed equally to this work.

0387-7604/$ - see front matter © 2012 The Japanese Society of Child Neurology. Published by Elsevier B.V. All rights reserved.
http://dx.doi.org/10.1016/j.braindev.2012.12.009

affects 0.31% of live newborn infants in Japan [2]. Approximately 10–15% of infants with congenital CMV infection (CCMVI) have clinical manifestations at birth such as jaundice, hepatosplenomegaly with or without liver dysfunction, thrombocytopenic purpura, chorioretinitis, and abnormalities of the central nervous system. Of such symptomatic infants, approximately 80–90% develop major neurological sequelae including sensorineural hearing loss (SNHL) and developmental disabilities [1].

Previous studies have shown that brain abnormalities, including intracranial calcification and ventricular dilatation (VD), are associated with the development of SNHL [3–5] and can be used to predict SNHL in infants with CCMVI [4,5]. Computed tomography (CT) images are still considered in infants with suspected CCMVI in the early postnatal period to rule out calcifications or VD of their brains, although magnetic resonance imaging (MRI) and ultrasound examinations have widely spread in Japan. VD has been generally assessed qualitatively (presence or absence of VD) or semi-quantitatively based on CT images (mild, moderate, or severe VD) [3–5]. However, because such assessment has yielded inconsistent results among pediatric radiologists [3], it is critical to establish a method for quantitative evaluation of ventricle size that can provide a more accurate marker of SNHL in infants with CCMVI.

Evans' index (EI), the ratio of the maximum width of the frontal horns of the lateral ventricles to the greatest internal diameter of the skull, is the most well-known index for quantitative evaluation of ventricle size on CT images [6]. International guidelines for the diagnosis of hydrocephalus define VD as EI > 0.3 [7,8]. The lateral ventricle width/hemispheric width (LVW/HW) ratio is the standard index used for evaluation of fetal VD on ultrasound examination [9–12]. No reported studies to date have used either EI or LVW/HW ratio to assess VD on CT images in infants with CCMVI.

The aims of this study were to establish a method for quantitative evaluation of ventricle size using CT images to obtain EI and LVW/HW ratio, and to determine cut-off values for EI and LVW/HW ratio associated with abnormal auditory brainstem response (ABR) in infants with CCMVI early in life.

2. Methods

2.1. Study design

This study was conducted from April 2009 to March 2012 at Kobe University Hospital. The collections and uses of human materials for this study were approved by the Ethical Committee of Kobe University Graduate School of Medicine. Written informed consent was obtained from the parents of the enrolled infants.

Infants of mothers who had confirmed or suspected primary CMV infection were enrolled in this study. All of them underwent blood testing, CMV-DNA analysis, brain CT, ABR evaluation, and ophthalmologic examination. CMV-DNA analysis was used to allocate infants to the CCMVI or control groups. The CCMVI group was divided into two subgroups according to ABR: CCMVI with normal ABR and CCMVI with abnormal ABR. The clinical background characteristics of all enrolled infants were recorded, including gestational age, birth weight, gender, initial physical examination findings, and postconceptional age at the time of brain CT and ABR evaluation. EI and LVW/HW ratio were obtained as shown in Fig. 1. Clinical background characteristics, EI, and LVW/HW ratio were compared among the groups (control, CCMVI, CCMVI with normal ABR, and CCMVI with abnormal ABR). Finally, cut-off values for EI and LVW/HW ratio associated with abnormal ABR were determined.

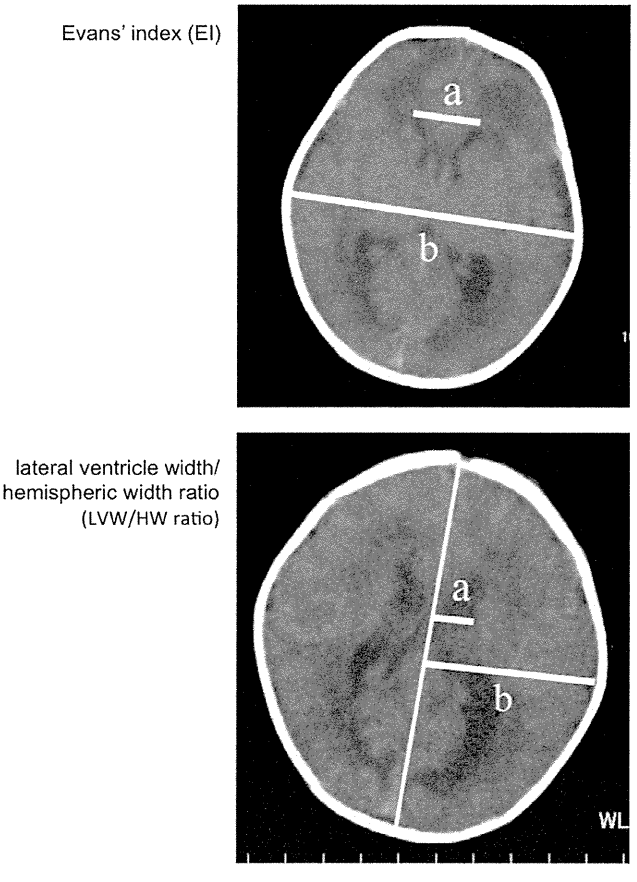

Fig. 1. Quantitative evaluations of ventricle size: Evans' index (EI) and lateral ventricle width/hemispheric width (LVW/HW) ratio. EI = maximum width of the frontal horns of the lateral ventricles (a)/internal diameter of the skull (b), LVW/HW ratio = maximum lateral ventricle width (a)/hemispheric width (b).

2.2. Diagnosis of CCMVI

Once pregnant mothers were confirmed or suspected primary CMV infection based on positive CMV-IgM and/or a low CMV-IgG avidity index (<45%) during pregnancy [13], the presence of CMV-DNA in urine specimens of their newborn infants within 1 week of birth was tested by the urine filter-based quantitative polymerase chain reaction (PCR) assay, and then was confirmed by the standard quantitative real-time PCR assay as previously described [2,14]. CCMVI of infants with more than 3 weeks of age was diagnosed if CMV-DNA was detected in a dried umbilical cord specimen using the real-time PCR assay as previously described [14,15].

2.3. Definitions of manifestations of CCMVI

Hepatosplenomegaly was confirmed by ultrasound examination and/or abdominal X-ray. Hepatitis was defined as serum alanine aminotransferase level >100 U/L, thrombocytopenia as platelet count $<1 \times 10^5\ \mu L^{-1}$, and jaundice as serum direct bilirubin level >2 mg/dL [4,16]. Chorioretinitis was diagnosed by a pediatric ophthalmologist. Intracranial calcification on brain CT images was diagnosed by a radiologist. ABR abnormality was diagnosed by using a Neuropack S1 (Nihon Kohden Co., Tokyo, Japan) according to the manufacturer's recommended protocol. A non-response to 40 dB for infants with a postconceptional age of $\geqslant$37 weeks and 50 dB for infants with a postconceptional age of 34–36 weeks was defined as abnormal, either unilaterally or bilaterally [17,18].

2.4. Brain CT images

All brain CT examinations were performed using a 64-slice multidetector CT scanner (Aquilion, Toshiba Medical Systems, Tokyo, Japan). The following technical parameters were used for CT scanning: 120 kV peak energy, 120 mA current with automated radiation exposure control, and 4-mm reconstruction thickness. CT images parallel to the orbitomeatal line were analyzed.

2.5. Quantitative evaluations of ventricle size

EI and LVW/HW ratio were used to quantitatively evaluate ventricle size (Fig. 1). An expert radiologist, who was blinded to detailed clinical findings, reviewed all CT scans. EI was calculated as the ratio of the maximum width of the frontal horns of the lateral ventricles to the largest internal diameter of the skull. The maximum width of the frontal horns was measured on the slice with the largest width, and the largest internal diameter of the skull was measured on the same slice [6]. LVW/HW ratio was calculated as the ratio of the maximum lateral ventricle width to the maximum hemispheric width on the left side. The maximum lateral ventricle width was measured on the slice with the largest width, and the maximum hemispheric width was measured on the same slice [9,10].

2.6. Statistical analysis

Statistical analyses were performed using the Mann–Whitney nonparametric rank test for comparison of two independent data sets. Differences were deemed statistically significant at $p < 0.05$. Cut-off values for EI and LVW/HW ratio associated with abnormal ABR were determined using receiver operating characteristic curve (ROC) analyses [19]. Sensitivity, specificity, negative predictive value, positive predictive value, and likelihood ratio for positive and negative results were calculated.

3. Results

3.1. Clinical background characteristics of enrolled infants

This study enrolled 19 infants in the CCMVI group and 21 infants in the control group. Of the 19 CCMVI infants, 18 were diagnosed by CMV-DNA detection in urine specimens and one was diagnosed by CMV-DNA detection in a dried umbilical cord specimen. Ten infants with CCMVI were asymptomatic and nine had some manifestations at the time of initial examination as follows: eight had abnormal ABR, four had hepatosplenomegaly, three had hepatitis, one had jaundice, two had thrombocytopenia with petechiae, two had chorioretinitis, and five had intracranial calcifications. Baseline characteristics of infants in the CCMVI and control groups are shown in Table 1. There were no significant differences in gestational age, birth weight, gender, or postconceptional age at the time of brain CT or ABR evaluation between these two groups. There were also no significant differences in gestational age, birth weight, gender, or postconceptional age at the time of brain CT or ABR evaluation between the CCMVI with normal ABR group ($n = 11$) and the CCMVI with abnormal ABR group ($n = 8$; five with bilateral and three with unilateral abnormality). No infants with abnormal ABR were found in the control group.

3.2. EI and LVW/HW ratio in infants without and with CCMVI

In infants without CCMVI, the median EI was 0.23 and the median LVW/HW ratio was 0.19 (Fig. 2).

Fig. 2 shows comparisons of EI and LVW/HW ratio between the CCMVI and control groups. EI and LVW/HW ratio were significantly higher in the CCMVI group

Table 1
Clinical background characteristics of enrolled infants.

	Control, $n = 21$	CCMVI		
		Total, $n = 19$	Normal ABR, $n = 11$	Abnormal ABR, $n = 8$
Gestational age (weeks)	38 (36–41)	38 (31–41)	38 (35–41)	37 (31–39)
Birth weight (g)	2822 (2218–3688)	2868 (1378–3840)	3074 (2362–3840)	2334 (1378–3160)
Male/female	9/12	6/13	3/8	3/5
Postconceptional age at the time of brain CT (weeks)	38 (36–42)	40 (34–52)	42 (38–45)	38 (34–52)
Postconceptional age at the time of ABR evaluation (weeks)	39 (36–42)	40 (34–48)	42 (39–45)	38 (34–48)

Data are expressed as median (range) or number. CCMVI = congenital cytomegalovirus infection; ABR = auditory brainstem response; CT = computed tomography.

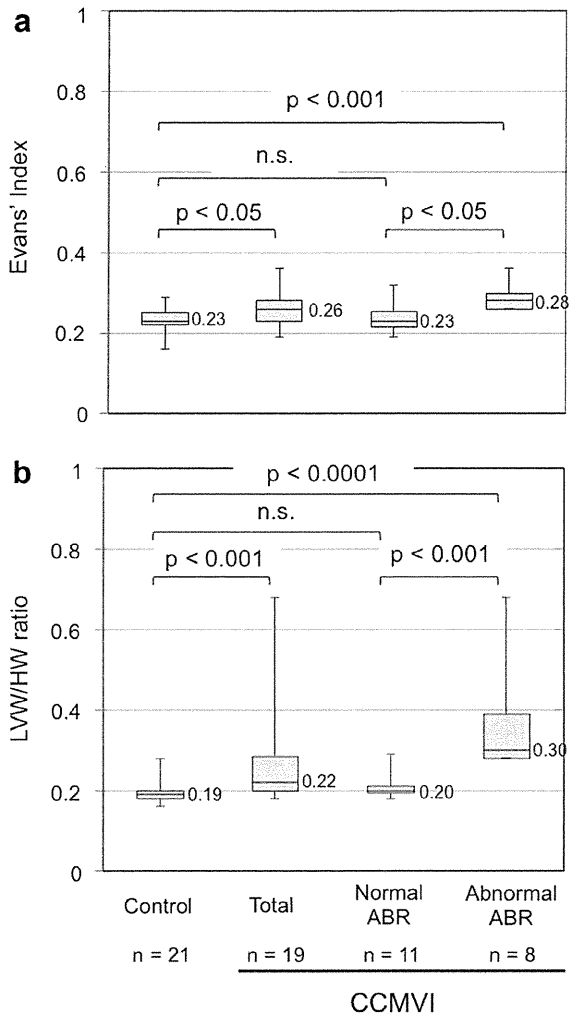

Fig. 2. Comparisons of Evans' index (a) and lateral ventricle width/hemispheric width (LVW/HW) ratio (b) between the congenital cytomegalovirus infection (CCMVI) and control groups. Data are expressed as median and range. ABR = auditory brainstem response. p-Values between any two groups are shown. n.s. = not significant.

than the control group ($p < 0.05$ for EI and $p < 0.001$ for LVW/HW ratio). EI and LVW/HW ratio were significantly higher in the CCMVI with abnormal ABR group than the control and CCMVI with normal ABR groups. However, there were no significant differences in EI or LVW/HW ratio between the control and CCMVI with normal ABR groups.

3.3. Cut-off values associated with abnormal ABR

EI and LVW/HW ratio in infants with CCMVI with normal or abnormal ABR were analyzed by ROC analyses (Fig. 3). Area under curve for EI and LVW/HW ratio was 0.847 and 0.955, respectively. The cut-off values associated with abnormal ABR were 0.26 for EI and 0.28 for LVW/HW ratio. The test performance characteristics were as follows. A cut-off value of 0.26 for EI had sensitivity of 100%, specificity of 72.7%, negative predictive value of 100%, positive predictive value of 72.7%, and likelihood ratio for positive and negative results of 3.67 and 0. A cut-off value of 0.28 for LVW/HW ratio had sensitivity of 100%, specificity of 90.9%, negative predictive value of 100%, positive predictive value of 88.9%, and likelihood ratio for positive and negative results of 11.0 and 0.

4. Discussion

This is the first study to report a method for quantitative evaluation of ventricle size using EI and LVW/HW ratio on brain CT in infants with CCMVI. We found that VD was associated with abnormal ABR in infants with CCMVI early in life. The cut-off values associated with abnormal ABR in infants with CCMVI were 0.26 for EI and 0.28 for LVW/HW ratio. Interestingly, LVW/HW ratio had a more association with abnormal ABR than EI.

We selected EI and LVW/HW ratio for quantitative evaluation of ventricle size, because these are the most popular indexes of VD in adult patients with hydrocephalus [6–8] and in fetuses [9–12]. Infants with and without CCMVI sometimes have asymmetrical ventricle sizes. We calculated LVW/HW ratios on the right and left sides in the CCMVI group, but found no significant dif-

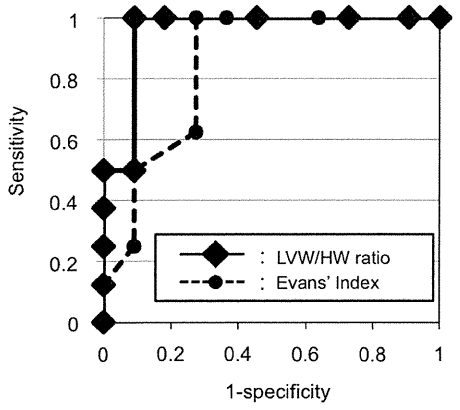

ABR

Evans' Index

	Abnormal	Normal	
≥ 0.26	8	3	11
< 0.26	0	8	8
	8	11	19

LVW/HW ratio

	Abnormal	Normal	
≥ 0.28	8	1	9
< 0.28	0	10	10
	8	11	19

Fig. 3. Receiver operating characteristic curve analyses of Evans' index (EI) and lateral ventricle width/hemispheric width (LVW/HW) ratio for associating with abnormal auditory brainstem response (ABR) in infants with congenital cytomegalovirus infection (CCMVI). The cut-off values were 0.26 for EI and 0.28 for LVW/HW ratio. LVW/HW ratio had a more association with abnormal ABR in infants with CCMVI than EI.

ference between sides (data not shown). LVW/HW ratio was therefore calculated only for the left side in this study.

To our knowledge, this is the first study reporting EI and LVW/HW ratio on brain CT in newborn infants with and without CCMVI. We suggest that EI and LVW/HW ratio can be used for quantitative evaluation of ventricle size, and for assessment of changes in ventricle size after treatment, in infants with CCMVI or other conditions causing VD such as intraventricular hemorrhage, congenital brain anomaly, or tumor. EI and LVW/HW ratio were significantly higher in infants with CCMVI with abnormal ABR than infants with CCMVI with normal ABR early in life. These data suggest that VD was associated with abnormal ABR in infants with CCMVI. Previous studies have reported that calcifications, cysts, white matter changes, or VD on CT or ultrasound examination predicted SNHL in infants with CCMVI [3–5]. CMV infection *in utero* may cause injury to the brain and inner ears, resulting in auditory nerve injury in infants with VD, although we have not known the mechanisms of their associations. On the other hand, Rivera et al. reported that the presence of microcephaly and other neurologic abnormalities was not predictive of SNHL including late-onset SNHL [20]. A reason for the difference between our and their results may be whether the study subjects include late-onset SNHL (30% and 0% of enrolled CCMVI patients in Rivera's and our reports) [20]. Further studies involving larger numbers of infants with CCMVI and VD are needed to confirm this association. The mechanisms for simultaneous incidence of VD and abnormal ABR also should be clarified.

We found that LVW/HW ratio had a more association with abnormal ABR in infants with CCMVI than EI. Neural stem cells are the predominant cell type in the fetal brain, and are located predominantly in the subventricular and subgranular zones of the hippocampus. These cells are damaged by CMV infection during fetal development [21]. In Alzheimer's disease, the hippocampus is one of the first regions of the brain to show damage. The size of the body of the lateral ventricle and LVW/HW ratio were found to be better predictors of Alzheimer's disease than the width between the frontal horns of the lateral ventricles or EI [22]. This study indicates that in infants with CCMVI, using EI as a marker of abnormal ABR is more likely to give false-positive results than using LVW/HW ratio.

CT scanning requires the additional risk and expense of transporting a seriously ill infant. It is already known that detection of VD is correlated between CT and ultrasound examinations [23]. Fetal ultrasound examination is routinely performed during pregnancy [9–12], and it has been reported that detection of VD using LVW/HW ratio in the fetus can assist with diagnosis of myelomeningocele or meningitis due to intrauterine infection in the early postnatal period [12]. We suggest that ultrasound evaluation of ventricle size using LVW/HW ratio in fetuses with CCMVI may be used as an early predictor of hearing impairment in the early postnatal period. Further studies are needed to investigate the association between ventricle size in fetuses with CCMVI and the development of abnormal ABR after birth.

The limitations of our study are as follows. First, abnormal ABR has not been proved to cause by VD alone in the previous reports [3–5]. Correlations between VD and other neurological symptoms, such as microcephaly, intracranial calcification and cortical dysplasia should be analyzed. However, we could not correctly assess their correlations as this study enrolled only a small number of infants with these neurological symptoms. Second, we investigated the association between VD on brain CT images and abnormal ABR in the early period after birth in this study. There are some reports that patients who were infected CMV during late pregnancy did not present VD, but showed progressive SNHL [24,25]. Because asymptomatic CCMVI infants

sometimes develop late-onset SNHL, long-term auditory outcomes are needed to investigate in this study subjects to show the association between VD on brain CT images and all congenital CMV-associated SNHL. Finally, because MRI provides more information of white matter lesions and malformations of cortical development in addition to VD and calcifications simultaneously, quantitative evaluation of ventricle size for CCMVI infants should be studied using MRI in the early postnatal period.

Conflict of interest

The authors have no financial or personal relations that could pose a conflict of interest.

Acknowledgments

This work was supported in part by Grants-in-Aid from the Ministry of Education, Culture, Sports, Science and Technology of Japan (I.M. and A.M.), the Ministry of Health, Labor and Welfare of Japan (H23-Jisedai-Ippan-001), and the Japan Association of Obstetricians and Gynecologists (H22, 23-Ogyah-Kenkin).

References

[1] Lazzarotto T, Lanari M. Why is cytomegalovirus the most frequent cause of congenital infection? Expert Rev Anti Infect Ther 2011;9:841–3.
[2] Koyano S, Inoue N, Oka A, Moriuchi H, Asano K, Ito Y, et al. Screening for congenital cytomegalovirus infection using newborn urine samples collected on filter paper: feasibility and outcomes from a multicentre study. BMJ Open 2011;1:e000118.
[3] Boppana SB, Fowler KB, Vaid Y, Hedlund G, Stagno S, Britt WJ, et al. Neuroradiographic findings in the newborn period and long-term outcome in children with symptomatic congenital cytomegalovirus infection. Pediatrics 1997;99:409–14.
[4] Noyola DE, Demmler GJ, Nelson CT, Griesser C, Williamson WD, Atkins JT, et al. Early predictors of neurodevelopmental outcome in symptomatic congenital cytomegalovirus infection. J Pediatr 2001;138:325–31.
[5] Ancora G, Lanari M, Lazzarotto T, Venturi V, Tridapalli E, Sandri F, et al. Cranial ultrasound scanning and prediction of outcome in newborns with congenital cytomegalovirus infection. J Pediatr 2007;150:157–61.
[6] Hanson J, Levander B, Liliequist B. Size of the intracerebral ventricles as measured with computer tomography, encephalography and echoventriculography. Acta Radiol Suppl 1975;346:98–106.
[7] Relkin N, Marmarou A, Klinge P, Bergsneider M, Black PM. Diagnosing idiopathic normal-pressure hydrocephalus. Neurosurgery 2005;57(Suppl.):S4–S16.
[8] Ishikawa M, Hashimoto M, Kuwana N, Mori E, Miyake H, Wachi A, et al. Guidelines for management of idiopathic normal pressure hydrocephalus. Neurol Med Chir (Tokyo) 2008;48(Suppl.):S1–S23.
[9] Jeanty P, Dramaix-Wilmet M, Delbeke D, Rodesch F, Struyven J. Ultrasonic evaluation of fetal ventricular growth. Neuroradiology 1981;21:127–31.
[10] D'Addario V, Kurjak A. Ultrasound investigation of the fetal cerebral ventricles. J Perinat Med 1985;13:67–77.
[11] Fiske CE, Filly RA, Callen PW. Sonographic measurement of lateral ventricular width in early ventricular dilation. J Clin Ultrasound 1981;9:303–7.
[12] Jörgensen C, Ingemarsson I, Svenningsen NW. Prenatal diagnosis of fetal brain ventricle dilatation. Br J Obstet Gynaecol 1983;90:162–6.
[13] Tagawa M, Minematsu T, Masuzaki H, Ishimaru T, Moriuchi H. Seroepidemiological survey of cytomegalovirus infection among pregnant women in Nagasaki, Japan. Pediatr Int 2010;52:459–62.
[14] Watzinger F, Suda M, Preuner S, Baumgartinger R, Ebner K, Baskova L, et al. Real-time quantitative PCR assays for detection and monitoring of pathogenic human viruses in immunosuppressed pediatric patients. J Clin Microbiol 2004;42:5189–98.
[15] Koyano S, Inoue N, Nagamori T, Yan H, Asanuma H, Yagyu K, et al. Dried umbilical cords in the retrospective diagnosis of congenital cytomegalovirus infection as a cause of developmental delays. Clin Infect Dis 2009;48:e93-5.
[16] Kimberlin DW, Lin CY, Sánchez PJ, Demmler GJ, Dankner W, Shelton M, et al. Effect of ganciclovir therapy on hearing in symptomatic congenital cytomegalovirus disease involving the central nervous system: a randomized, controlled trial. J Pediatr 2003;143:16–25.
[17] Coenraad S, Toll MS, Hoeve HL, Goedegebure A. Auditory brainstem response morphology and analysis in very preterm neonatal intensive care unit infants. Laryngoscope 2011;121:2245–9.
[18] Wong V, Chen WX, Wong KY. Short- and long-term outcome of severe neonatal nonhemolytic hyperbilirubinemia. J Child Neurol 2006;21:309–15.
[19] Metz CE, Herman BA, Roe CA. Statistical comparison of two ROC-curve estimates obtained from partially-paired datasets. Med Decis Making 1998;18:110–21.
[20] Rivera LB, Boppana SB, Fowler KB, Britt WJ, Stagno S, Pass RF. Predictors of hearing loss in children with symptomatic congenital cytomegalovirus infection. Pediatrics 2002;110:762–7.
[21] Cheeran MC, Lokensgard JR, Schleiss MR. Neuropathogenesis of congenital cytomegalovirus infection: disease mechanisms and prospects for intervention. Clin Microbiol Rev 2009;22:99–126.
[22] Albert M, Naeser MA, Levine HL, Garvey AJ. Ventricular size in patients with presenile dementia of the Alzheimer's type. Arch Neurol 1984;41:1258–63.
[23] Skolnick ML, Rosenbaum AE, Matzuk T, Guthkelch AN, Heinz ER. Detection of dilated cerebral ventricles in infants: a correlative study between ultrasound and computed tomography. Radiology 1979;131:447–51.
[24] Steinlin MI, Nadal D, Eich GF, Martin E, Boltshauser EJ. Late intrauterine cytomegalovirus infection: clinical and neuroimaging findings. Pediatr Neurol 1996;15:249–53.
[25] Rosenthal LS, Fowler KB, Boppana SB, Britt WJ, Pass RF, Schmid SD, et al. Cytomegalovirus shedding and delayed sensorineural hearing loss: results from longitudinal follow-up of children with congenital infection. Pediatr Infect Dis J 2009;28:515–20.

LETTERS

Newborn screening of congenital cytomegalovirus infection using saliva can be influenced by breast feeding

Congenital cytomegalovirus (cCMV) infection occurs in 0.2–2% of all births in developed countries and causes developmental abnormalities.[1] In addition to patients symptomatic at birth, asymptomatic newborns can develop late-onset sequelae, including sensorineural hearing loss and developmental delay. As the early identification of congenitally infected newborns may allow early intervention and antiviral treatment options, it is important to establish newborn cCMV screening programmes.

Since newborn screening assays using dried blood spots for cCMV infection were shown to have a limitation in their sensitivity, Boppana *et al*[2] reported an alternative assay using saliva specimen last year. Even with a consideration of CMV secretions into the breast milk of carrier mothers, the overall frequency of false-positive results for their saliva-based PCR assay was reported to be less than 0.03%. However, there remains a concern that carry-over from breast milk may generate false-positive results as CMV appears in breast milk within a few days after parturition.[3]

To validate their assay, we examined the presence of CMV DNA in breast milk and saliva specimens that were collected, with informed consent, within 6 days after parturition from 11 mothers and their newborns (table 1). Two of the mothers were found to have secreted CMV into their breast milk that was collected a few times after parturition. Two saliva specimens collected within 30 min after breast-feeding were CMV positive, although none of those collected before feeding contained detectable levels of CMV. CMV strains isolated from baby No.1's saliva specimens and her mother's breast milk were found to be identical by sequencing their genomes.

These results suggest that the timing of specimen collection is critical to ensure proper implementation of saliva-based screening programmes. Alternatively, CMV screening can be done by collecting urine onto filter paper placed in diaper, as we reported recently.[4]

Shin Koyano,[1] Naoki Inoue,[2] Tsunehisa Nagamori,[1] Hiroyuki Moriuchi,[3] Hiroshi Azuma[1]

[1]Department of Paediatrics, Asahikawa Medical University, Asahikawa, Japan
[2]Department of Virology I, National Institute of Infectious Diseases, Tokyo, Japan
[3]Department of Paediatrics, Nagasaki University, Nagasaki, Japan

Correspondence to Dr Shin Koyano, Department of Paediatrics, Asahikawa Medical University, Midorigaoka-Higashi 2-1-1-1, Asahikawa 078-8510, Japan; koyano5p@asahikawa-med.ac.jp

Acknowledgements The authors thank H. Hidaka, M. Ishikawa and all medical staff of the Ai Women's Clinic for their assistance with specimen collection.

Funding This work was supported by Grants for the Research on Child Development and Diseases (H23-Jisedai-Ippan-001) from the Ministry of Health, Labor and Welfare, Japan.

Competing interests None.

Patient consent Obtained.

Ethics approval Asahikawa Medical University.

Provenance and peer review Not commissioned; externally peer reviewed.

Table 1 Detection of cytomegalovirus (CMV) DNA in breast milk, saliva, and urine specimens

Baby No.	Days after parturition	Breast milk	Saliva		Urine
			After feeding	Before feeding	
1	3	+	+	–	–
2	3	–	+	–	–
3	3	–	–	–	–
4	4	–	–	–	–
5	3	–	–	–	–
6	5	–	–	–	–
7	2	+	–	–	–
8	4	–	–	–	–
9	3	–	–	–	–
10	4	–	–	–	–
11	6	–	–	–	–

+, CMV DNA-positive; –, CMV DNA-negative.

To cite Koyano S, Inoue N, Nagamori T, *et al*. *Arch Dis Child Fetal Neonatal Ed* 2013;**98**:F182.

Received 20 April 2012
Revised 20 April 2012
Accepted 18 June 2012
Published Online First 8 August 2012

Arch Dis Child Fetal Neonatal Ed 2013;**98**:F182.
doi:10.1136/archdischild-2012-302230

REFERENCES

1 Pass RF. Cytomegalovirus. In: Knipe DM, Howley PM, eds. 4th edn. Philadelphia, PA: Lippincott Williams & Wilkins, 2001:2675–705.
2 Boppana SB, Ross SH, Shimamura M, *et al*. Saliva polymerase–chain-reaction assay for cytomegalovirus screening in newborns. *N Engl J Med* 2011;364:2111–18.
3 Hamprecht K, Maschmann J, Vochem M, *et al*. Epidemiology of transmission of cytomegalovirus from mother to preterm infant by breastfeeding. *Lancet* 2001;357:513–18.
4 Koyano S, Inoue N, Oka A, *et al*. Screening for congenital cytomegalovirus infection using newborn urine samples collected on filter paper: feasibility and outcomes from a multi-centre large-scale study. *BMJ Open* 2011;1:e000118.

Newborn screening of congenital cytomegalovirus infection using saliva can be influenced by breast feeding

Shin Koyano, Naoki Inoue, Tsunehisa Nagamori, et al.

Arch Dis Child Fetal Neonatal Ed 2013 98: F182 originally published online August 8, 2012
doi: 10.1136/archdischild-2012-302230

Nakamura et al. Herpesviridae 2013, 4:2
http://www.herpesviridae.org/content/4/1/2

HERPESVIRIDAE

RESEARCH Open Access

Human cytomegalovirus induces apoptosis in neural stem/progenitor cells derived from induced pluripotent stem cells by generating mitochondrial dysfunction and endoplasmic reticulum stress

Hiroyuki Nakamura[1*], Huanan Liao[1], Kahori Minami[2], Masashi Toyoda[2], Hidenori Akutsu[2], Yoshitaka Miyagawa[3], Hajime Okita[3], Nobutaka Kiyokawa[3], Akihiro Umezawa[2], Ken-Ichi Imadome[1], Naoki Inoue[4] and Shigeyoshi Fujiwara[1]

Abstract

Background: Congenital human cytomegalovirus (HCMV) infection, a leading cause of birth defects, is most often manifested as neurological disorders. The pathogenesis of HCMV-induced neurological disorders is, however, largely unresolved, primarily because of limited availability of model systems to analyze the effects of HCMV infection on neural cells.

Methods: An induced pluripotent stem cell (iPSC) line was established from the human fibroblast line MRC5 by introducing the Yamanaka's four factors and then induced to differentiate into neural stem/progenitor cells (NSPCs) by dual inhibition of the SMAD signaling pathway using Noggin and SB-431542.

Results: iPSC-derived NSPCs (NSPC/iPSCs) were susceptible to HCMV infection and allowed the expression of both early and late viral gene products. HCMV-infected NSPC/iPSCs underwent apoptosis with the activation of caspase-3 and −9 as well as positive staining by the terminal deoxynucleotidyl transferase-mediated dUTP nick-end labeling (TUNEL). Cytochrome c release from mitochondria to cytosol was observed in these cells, indicating the involvement of mitochondrial dysfunction in their apoptosis. In addition, phosphorylation of proteins involved in the unfolded protein response (UPR), such as PKR-like eukaryotic initiation factor 2a kinase (PERK), c-Jun NH2-terminal kinase (JNK), inositol-requiring enzyme 1 (IRE1), and the alpha subunit of eukaryotic initiation factor 2 (eIF2α) was observed in HCMV-infected NSPC/iPSCs. These results, coupled with the finding of increased expression of mRNA encoding the C/EBP-homologous protein (CHOP) and the detection of a spliced form of X-box binding protein 1 (XBP1) mRNA, suggest that endoplasmic reticulum (ER) stress is also involved in HCMV-induced apoptosis of these cells.

Conclusions: iPSC-derived NSPCs are thought to be a useful model to study HCMV neuropathogenesis and to analyze the mechanisms of HCMV-induced apoptosis in neural cells.

Keywords: Human cytomegalovirus, iPS cells, Neural stem/progenitor cells, Apoptosis, ER stress

* Correspondence: nakamura-hry@ncchd.go.jp
[1]Department of Infectious Diseases, National Research Institute for Child Health and Development, 2-10-1 Okura, Setagaya-ku, Tokyo 157-8535, Japan
Full list of author information is available at the end of the article

Background

Congenital cytomegalovirus (CMV) infection is a major cause of birth defects resulting mainly from primary CMV infection during pregnancy. At birth, approximately 5 to 10% of congenitally infected newborns are estimated to be symptomatic exhibiting multi-organ disorders including neurological defects such as mental retardation, sensorineural hearing loss, and microencephaly [1,2]. A latest study showed that if laboratory findings including those from magnetic resonance imaging (MRI) images of the brain are considered, up to 30% of congenitally infected newborns exhibit some abnormal signs [3]. Sixty to 90% of congenitally infected children who are symptomatic at birth, and 10 to 15% of those who are asymptomatic at birth develop one or more long-term sequelae. Although CMV infects a wide variety of cell types, infection of the nervous system gives most serious and long-lasting damages to the host.

As a part of understanding the HCMV neuropathogenesis, it is important to scrutinize the cellular response to CMV infection in neural cells. Some human neural cell lines can be infected with HCMV with different permissiveness to HCMV gene expression and replication [4-7]. A recent study has shown that neural progenitor cells isolated from developing human brain tissues are susceptible to CMV infection and undergo apoptosis following infection [8,9]. However, the amount of neural cells obtainable from human brain tissues is limited.

Pluripotent stem cells, including embryonic stem cells (ESCs) and induced pluripotent stem cells (iPSCs), are characterized by the ability to differentiate into tissues derived from any of the three embryonic germ layers. Recent advances in the method to induce efficient differentiation of either ESCs or iPSCs into specific cell lineages offer an opportunity to establish model systems for viral infections of various cell types, including neural cells. Furthermore, differentiated cells derived from pluripotent stem cells are obtainable in potentially unlimited amounts. Previous works revealed that while mouse ESCs are not susceptible to murine CMV (MCMV), NSPCs that are differentiated from them are susceptible and their proliferation and differentiation are suppressed by MCMV [10-13]. Experiments with human ESCs are, however, complicated with ethical problems.

In this study, to analyze the pathological effects of HCMV on neural cells, we prepared NSPCs from human iPSCs and examined whether NSPCs are susceptible to HCMV infection. The results indicated that NSPCs are susceptible to HCMV infection and undergo apoptosis caused by mitochondrial dysfunction and endoplasmic reticulum (ER) stress.

Methods

Cells and viruses

The human fetal lung fibroblast MRC5 was grown in Dulbecco's modified Eagle's medium (DMEM) supplemented with 10% fetal bovine serum (FBS; Invitrogen, Carlsbad, CA). The human foreskin fibroblast cell line hTERT-BJ1 immortalized with the human telomerase reverse transcriptase (Clontech, Palo Alto, CA) was grown in a medium consisting of 4 parts of DMEM and 1 part of medium 199 (Sigma) supplemented with 10% FBS, 1 mM sodium pyruvate (Sigma), and 2 mM glutamine (Invitrogen). HCMV laboratory strain Towne (ATCC VR-977) was propagated in hTERT-BJ1 cells. The human iPSC line MRC-iPS-25 that was established from MRC5 by retroviral vector-mediated transduction of the c-Myc, Oct-4, Klf4, and Sox2 genes [14,15] were cultured on mitomycin C-treated mouse embryonic fibroblasts (MEFs) in an iPSC medium consisting of Knockout DMEM/F12 (Invitrogen) supplemented with non-essential amino acids (0.1 mM, Invitrogen), glutamax I (1 mM, Invitrogen), 20% Knockout Serum Replacement (Invitrogen), β-mercaptoethanol (55 μM, Invitrogen) and basic fibroblast growth factor (10 ng/mL; Peprotech, Rocky Hill, NJ).

Induced differentiation on iPSCs into neural stem cells

MRC-iPSC-25 cells cultured under feeder-free conditions were induced to differentiate into neural stem/progenitor cells (NSPCs) by the method of dual inhibition of the SMAD signaling pathway described previously [16]. In brief, feeder-free iPSCs were treated with the mTeSR1 medium (StemCell Technologies, Vancouver, BC, Canada) containing Y27632 (Wako Pure Chemicals, Osaka, Japan) and maintained with a daily medium change for 4 days. Then the medium was replaced with iPSC medium supplemented with SB431542 (10 nM, Wako Pure Chemicals) and Noggin (500 ng/ml, Wako Pure Chemicals). This date was designated day 0. On day 2, culture medium was replaced with a medium consisting of 3 parts of iPSC medium and 1 part of N2 medium (Knockout DMEM/F12 containing 1× N2 supplement) supplemented with SB431542 (10 nM) and Noggin (500 ng/ml). On day 4, culture medium was replaced with a medium consisting of 1 part of iPSC medium and 1 part of N2 medium supplemented with SB431542 (10 nM) and Noggin (500 ng/ml). On day 6, cells were expanded in StemPro NSC SFM (Invitrogen). MRC-iPSC-25 cells cultured under feeder-free conditions and NSPC/iPSCs were infected with the Towne strain HCMV at a multiplicity of infection (MOI) of 1 plaque forming unit (PFU) per cell. To detect infectious virions produced from HCMV-infected NSPC/iPSCs, supernatant was collected and replaced with fresh medium every two days after infection. hTERT-BJ1 cells were inoculated with the supernatant and examined by IFA for expression of IE1/IE2.

Antibodies

Antibodies used were as follows: rabbit anti-Sox2, rabbit anti-Nanog, rabbit anti-Oct-4, rabbit anti-cleaved caspase-

3, rabbit anti-cleaved caspase-9, rabbit anti-phospho-eIF2α (Ser51), rabbit anti-phospho-PERK (Thr980), and rabbit anti-phospho-SAPK/JNK (Thr183/Tyr185)(Cell Signaling Technology, Beverly, MA); mouse anti-CMV IE1/IE2, rabbit anti-Musashi-1, and rabbit anti-cytochrome c (Millipore, Temecula, CA); rabbit anti-Nestin and mouse anti-α-tubulin (Sigma-Aldrich, St. Louis, MO); rabbit anti-Pax6 (Covance, Princeton, NJ), mouse anti-CMV gB (Abcam, Cambridge, MA); mouse anti-pp65 (Virusys Corporation, Sykesville, MD); rabbit anti-phosphorylated IRE1α (Pierce/Thermo Scientific, Rockford, IL); Alexa Fluor 488-conjugated goat anti-mouse IgG and Alexa Fluor 594-conjugated goat anti-rabbit IgG (Molecular Probes, Eugene, OR); horseradish peroxidase-conjugated donkey anti-rabbit IgG and horseradish peroxidase-conjugated sheep anti-mouse IgG (GE Healthcare, UK).

Immunofluorescence microscopy and immunoblot analysis

Cells were fixed with 4% parafolmaldehyde in PBS (Wako chemicals) at room temperature (RT) for 15 min. After fixation, cells were treated with 1.0% Triton X-100 in PBS for 15 min at RT and blocked with 10% goat serum in PBS for 30 min. Cells were incubated with the primary antibody at 4°C overnight, followed by washing in PBS and incubation with the corresponding secondary antibody at 37°C for 1 h. Nuclei were stained with DAPI. For the assessment of cell death, terminal deoxynucleotidyl transferase (TdT)-mediated dUTP nick-end labeling (TUNEL) assay was performed according to the manufacturer's instructions (Roche). Immunoblot analyses were performed as described previously [17].

Reverse transcriptase (RT)-PCR and real-time quantitative RT-PCR

Total RNA was isolated from mock- or HCMV-infected cells using TRIzol reagent (Invitrogen). Reverse transcription was performed on each RNA sample (5 μg) using SuperScript III First-Strand Synthesis System for RT-PCR (Invitrogen). Primer sequences are shown in Table 1. RT-PCR products were resolved by electrophoresis on 2% agarose gel and then visualized by ultraviolet illumination after ethidium bromide staining. Real-time quantitative RT-PCR was performed using TaqMan™ Universal Master Mix II with UNG (Applied Biosystems) on a StepOne Plus PCR System (Applied Biosystems). Amplifications were achieved in a final volume of 25 μl containing TaqMan probes labeled with FAM on the 5'-end and MGB on the 3'-end. The primers and probes for *UL136* were: forward primer, 5'-GGCCGTTGAAC GGAGCTAT-3' and reverse primer, 5'-CCATTTCCAC CGTGTCGAA-3', and TaqMan probe, 5'-FAM-TACT ACGGCAGCGGCT-MGB-3'. The forward and reverse primers and reporter probes for HCMV *IE1*, *UL89*, and Human *G6PD* were described previously [18].

Table 1 List of primer sequences for RT-PCR

Gene	Forward primer	Reverse primer
IE1*	ATGGAGTCCTCTGCCAAGAG	ATTCTATGCCGCACCATGTCC
IE2*	ATGGAGTCCTCTGCCAAGAG	CTGAGACTTGTTCCTCAGGTCCTG
vIL-10*	ATGCTGTCGGTGATGGTCTCTTCC	CTTTCTCGAGTGCAGATACTCTTCG
UL36*	GACCTACGGGACACGCTGATG	TGTGGAAGTGGTCGCAGTGAC
UL38	GACTACGACCACGCATAGCA	GGGAACAGAGCGTTCCAATA
pp65	CGCAACCTGGTGCCCATGG	CGTTTGGGTTGCGCAGCGGG
Nanog*	GCTTGCCTTGCTTTGAAGCA	TTCTTGACCGGGACCTTGTC
Oct-4	GAGCAAAACCCGGAGGAGT	TTCTCTTTCGGGCCTGCAC
Sox1	GCGGAAAGCGTTTTCTTTG	TAATCTGACTTCTCCTCCC
Sox2	ATGCACCGCTACGACGTGA	CTTTTGCACCCCTCCCATTT
Pax6*	AACAGACACAGCCCTCACAAACA	CGGGAACTTGAACTGGAACTGAC
Nestin*	CAGCGTTGGAACAGAGGTTGG	TGGCACAGGTGTCTCAAGGGTAG
MAP2*	CCACCTGAGATTAAGGATCA	GGCTTACTTTGCTTCTCTGA
GFAP*	GTACCAGGACCTGCTCAAT	CAACTATCCTGCTTCTGCTC
OSP*	ACTGCTGCTGACTGTTCTTC	GTAGAAACGGTTTTCACCAA
XBP1*	CCTTGTAGTTGAGAACCAGG	GGGGCTTGGTATATATGTGG
CHOP*	TGGAAGCCTGGTATGAGGAC	TCACCATTCGGTCAATCAGA
β-actin*	ACCATGGATGATGATATCGC	TCATTGTAGAAGGTGTGGTG
GAPDH*	CCACCCATGGCAAATTCCATGGCA	TCTAGACGGCAGGTCAGGTCCACC

Asterisks (*) indicate that amplified fragments contain splicing junctions. Amplified fragments for UL38, pp65, Oct-4, Sox1, and Sox2 did not contain splicing junctions, and therefore control experiments without reverse transcriptase confirmed the RNA origin of the PCR products.

Results

Preparation of human iPSC-derived neural stem/progenitor cells

Figure 1A demonstrates that MRC-iPS-25 cells have a typical iPSC colony morphology. The expression of pluripotency markers of iPSCs such as Nanog and Oct-4 in MRC-iPS-25 cells was confirmed by indirect immunofluorescence assay (IFA) (Figure 1B). The HCMV-encoded proteins IE1/IE2 were not detected in MRC-iPS-25 cells following inoculation with the virus, indicating that MRC-iPS-25 cells are either not susceptible to HCMV infection or do not support expression of the IE genes (Figure 1B).

NSPC/iPSCs prepared by induced differentiation of MRC-iPS-25 cells proliferated in a monolayer and displayed a rounded, immature neural morphology (Figure 1A). IFA (Figure 1C) showed that NSPC/iPSCs expressed the NSC markers Nestin, Sox2, and Pax6, indicating that NSPC/iPSCs have the authentic NSPC phenotype.

In vitro HCMV infection of iPSC-derived NSPCs

To examine the susceptibility of NSPC/iPSCs to HCMV infection, these cells were inoculated in vitro with the HCMV Towne strain at an MOI of 1 PFU per cell (Figure 2A). On the second day post-infection (dpi), NSPC/iPSCs started to show morphological changes including increased cell volume and cell fusion, and the number of cells with these

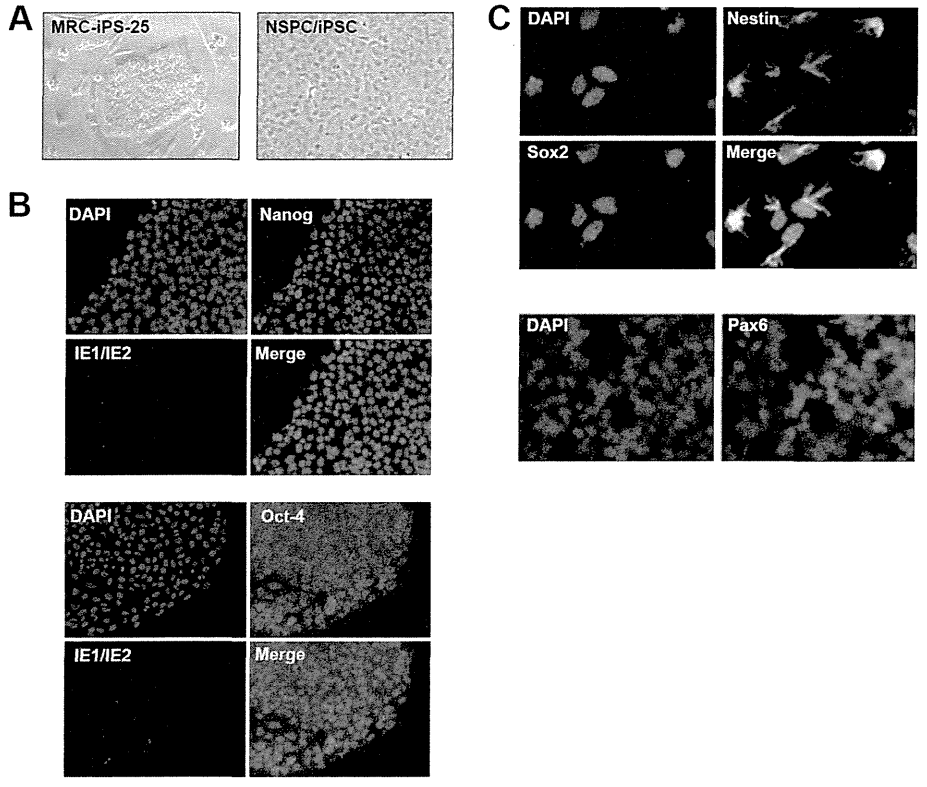

Figure 1 Differentiation of MRC-iPS-25 cells to neural stem/progenitor cells. (A) Phase-contrast images of MRC-iPS-25 cells cultured on a feeder layer of MEFs (left) and NSPC/iPSCs (right). **(B)** Immunofluorescence analysis of Towne-infected MRC-iPS-25 cells cultured under feeder-free conditions at 2 dpi stained with primary antibodies for pluripotent markers (Nanog or Oct-4) and HCMV IE1/IE2 proteins. Antigen proteins were detected with Alexa Fluor 488-conjugated goat anti-mouse IgG or Alexa Fluor 594-conjugated goat anti-rabbit IgG antibody. Nuclei were stained with DAPI. **(C)** Immunofluorescence analysis of NSPC markers Nestin, Sox2, and Pax6 in NSPC/iPSCs. NSPC/iPSCs were fixed and reacted with anti-Nestin (green), anti-Sox2 (red), and anti-Pax6 (red) antibodies, followed by detection with secondary antibodies. Immunofluorescence signals were obtained using a fluorescence microscope IX71. Representative results from three independent experiments are shown.

changes increased until 7 dpi (Figure 2A). To examine whether NSPC/iPSCs were capable of supporting HCMV gene expression, total RNA extracted from the infected NSPC/iPSCs was analyzed by RT-PCR. As shown in Figure 2B, mRNAs encoding IE1, IE2, vIL-10, and pp65 as well as those encoding HCMV anti-apoptotic proteins, such as UL36 and UL38, were detected. The kinetics of HCMV gene expression was analyzed by quantitative real-time RT-PCR (Figure 2C). IE1 mRNA was detected first on 1 dpi and increased steadily until 5 dpi. mRNAs for UL89 and UL136 were detected somewhat later and increased gradually until 7 dpi. The results showed the NSPC/iPSCs are susceptible to HCMV infection and allow the expression of several viral genes of both early and late functions.

Expression of HCMV genes in NSPC/iPSCs was evaluated at the protein level by immunoblot analysis on day 1, 2, 5, and 7 following HCMV infection. As shown in Figure 2D, the immediate-early protein IE1 was first detected at 1 dpi and its level increased until 5 dpi. Another immediate-early protein IE2 was detected a little later, becoming visible at 5 dpi. The expression of the HCMV lower matrix protein pp65 (ppUL83), already visible at 1 dpi, was markedly elevated at 5 and 7 dpi. The HCMV envelope glycoprotein B (gB; UL55) was detected at 5 to 7 dpi. Thus the expression of HCMV proteins of both immediate-early and late functions was demonstrated in NSPC/iPSCs.

We next examined the expression of cellular mRNAs encoding the pluripotency and neural differentiation markers (Figure 2E). Expression of the iPSC markers Nanog and Oct-4 remained at low levels following infection with HCMV, although that of Nanog tapered. While expression of the NSPC markers Sox2 and Pax6 were kept at high levels following HCMV infection, that of another NSPC marker Nestin was markedly suppressed at 7 dpi. In addition, expression of the neuronal marker microtubule-associated protein 2 (MAP2), the astrocyte marker glial fibrillary acidic protein (GFAP), and the oligodendrocyte marker oligodendrocyte-specific protein (OSP) was detected at low levels. Interestingly, Sox1, a marker specific to the neuroectodermal lineages [19], was markedly upregulated following infection with HCMV. Expression of the NSPC markers was evaluated

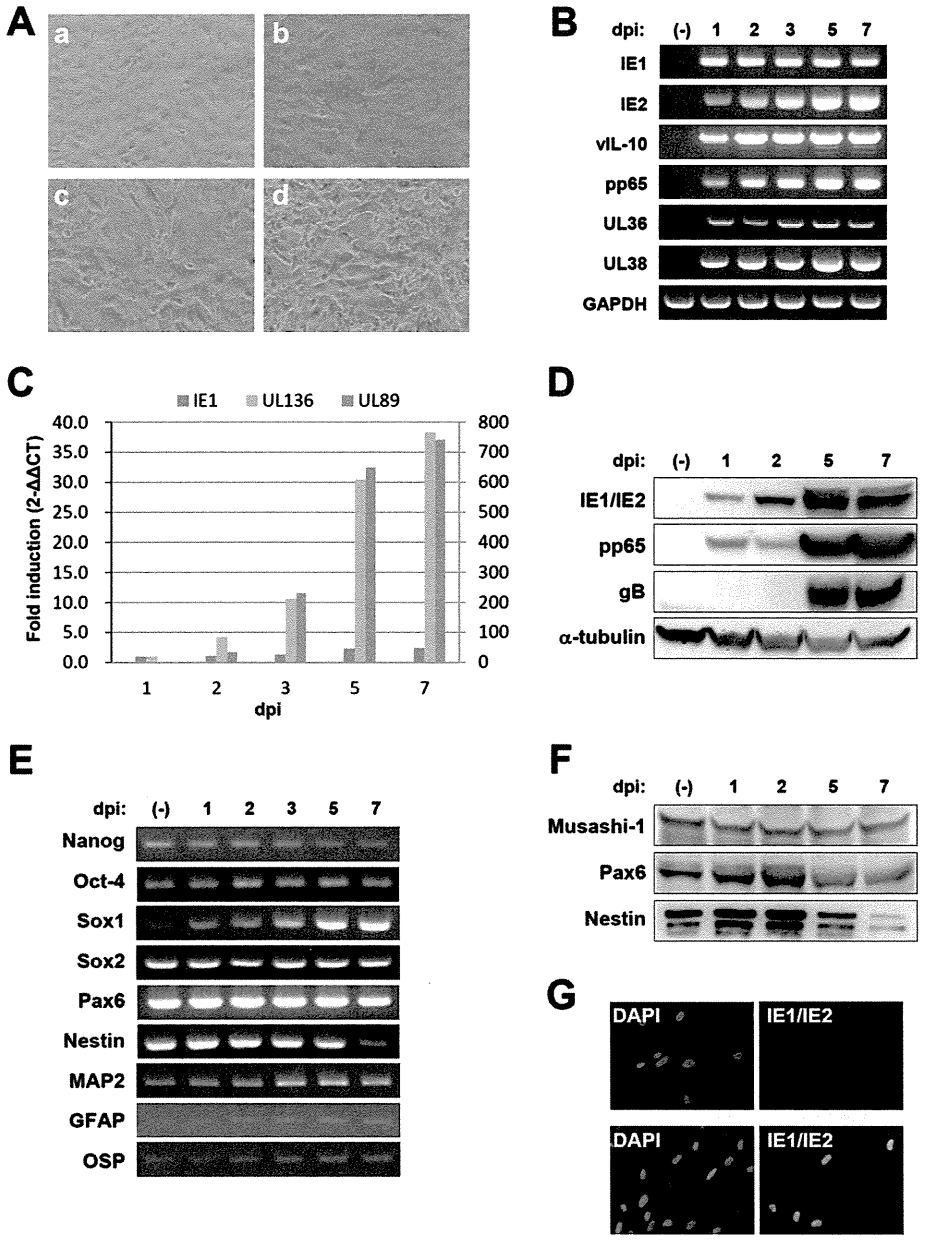

Figure 2 Analysis on the expression of viral and cellular gene products in NSPC/iPSCs. (A) Morphological changes of Towne-infected NSPC/iPSCs were observed under the inverted microscope before infection **(a)**, 2 dpi **(b)**, 5 dpi **(c)**, and 7 dpi **(d)**. **(B)** RT-PCR analysis of HCMV-encoding gene expression. Total RNAs isolated from NSPC/iPSCs harvested before (–) HCMV infection or at 1, 2, 3, 5, and 7 dpi with HCMV Towne strain were subjected to RT-PCR assays. GAPDH gene expression was assayed for the control. **(C)** The kinetics of mRNA expression for IE1, UL89, and UL136 in Towne-infected NSPC/iPSCs was examined by real-time quantitative RT-PCR assay. The mRNA expression was normalized to that of G6PDH gene. Real-time PCR data was analyzed by the 2-ΔΔCT method. The fold induction was calculated as the ratio of mRNA levels detected at each time point to that detected at 1 dpi. The y-axis represents fold induction of IE1 and UL136 mRNA (left y-axis) and UL89 mRNA (right y-axis). **(D)** Immunoblot analysis of HCMV protein expression in HCMV-infected NSPC/iPSCs. Whole-cell lysates of NSPC/iPSCs harvested before (–) HCMV infection or at 1, 2, 5, and 7 dpi with HCMV Towne strain were separated by SDS-PAGE and analyzed by immunoblotting with antibodies against IE1/IE2, pp65, gB, and α-tubulin. **(E)** RT-PCR analysis of pluripotency and neural differentiation marker gene expression in HCMV-infected NSPC/iPSCs. **(F)** Immunoblot analysis of neural differentiation marker protein expression in HCMV-infected NSPC/iPSCs. Whole-cell lysates of NSPC/iPSCs were analyzed by immunoblotting with antibodies against Musashi-1, Pax6, and Nestin. **(G)** hTERT-BJ1 cells inoculated with culture supernatant collected from mock-infected NSPC/iPSCs (upper panel) or Towne HCMV-infected NSPC/iPSCs (lower panel) at 8 dpi were subjected to immunofluorescence test with anti-IE1/IE2 antibody (green). Nuclei were stained with DAPI. Representative results from two independent experiments are shown.

also at the protein level by immunoblot analysis on 1, 2, 5, and 7 dpi (Figure 2F). In accordance with the results with RT-PCR, expression of Pax6 and Nestin was confirmed, and that of Nestin was found markedly decreased 7 dpi. Another NSPC marker Musashi-1 was also detected. To examine whether HCMV-infected NSPC/iPSCs produce infectious virions, culture supernatants collected from Towne HCMV-infected NSPC/iPSCs were inoculated to hTERT-BJ1 cells. Inoculated cells expressed IE1/IE2 indicating that infectious virions were produced from HCMV-infected NSPC/iPSCs (Figure 2G). The supernatant contained 30 PFU/mL of HCMV at 4, 6, 8 dpi, while no plaque forming virus was detected at 2 dpi.

HCMV infection induces apoptosis in iPSC-derived NSPCs

To examine whether HCMV infection in NSPC/iPSCs induces apoptotic responses, we performed the TUNEL assay combined with IFA using an antibody specific to HCMV gB. As shown in Figure 3A, NSPC/iPSCs expressing gB was positive for TUNEL staining and those without gB expression was consistently negative. We also performed IFA to analyze the activation status of caspases using antibodies specific to the activated forms of caspase-3 and caspase-9. The results show that the activated forms of caspase-3 and caspase-9 were specifically detected in more than 80% of HCMV-infected NSPC/iPSCs expressing IE1/IE2 proteins (Figure 3B and 3C), but not in mock-infected NSPC/iPSCs (Figure 3E). To see whether mitochondrial dysfunction is involved in the activation of caspase 9, intracellular distribution of cytochrome c was analyzed in HCMV-infected cells by IFA. As shown in Figure 3D and 3E, strong signals of cytochrome c were detected in the cytosol of cells expressing IE1/IE2 proteins, while only faint signals of cytochrome c were detected in cells not expressing IE1/IE2 proteins or in mock-infected cells. These results indicate that HCMV infection of NSPC/iPSCs activated apoptotic responses involving release of mitochondrial cytochrome c and serial activation of caspases.

Unfolded protein response in HCMV-infected NSPC/iPSCs

The unfolded protein response (UPR), induced by the accumulation of improperly folded proteins within the ER lumen (ER stress), is associated with multiple cellular responses such as neurodegeneration and apoptosis. ER stress sensor molecules, such as PKR-like eukaryotic initiation factor 2a kinase (PERK) and inositol-requiring enzyme 1 (IRE1), are activated on UPR and engage downstream signaling pathways. To examine whether the caspase-9 activation in HCMV-infected NSPC/iPSCs (Figure 3C) is associated with UPR, we analyzed phosphorylation status of IRE1α and its downstream target c-Jun NH2-terminal kinase (JNK) in immunofluorescence assays. Both IRE1α and JNK were specifically phosphorylated in HCMV-infected NSPC/iPSCs (Figure 4A and 4B), but not in mock-infected NSPC/iPSCs (Figure 4C). In concordance with the previous reports that activated IRE1α catalyzes the non-conventional splicing of the mRNA encoding X-box binding protein 1 (XBP1) [20,21], the spliced XBP1 mRNA increased gradually after HCMV infection in NSPC/iPSCs (Figure 4D). We also analyzed phosphorylation status of another sensor molecule PERK, an ER-associated serine/threonine protein kinase, and its downstream target the alpha subunit of eukaryotic initiation factor 2 (eIF2α). Phosphorylated forms of PERK and eIF2α were specifically detected in HCMV-infected NSPC/iPSCs (Figure 4E and 4F), but not in mock-infected NSPC/iPSCs (Figure 4G). The transcription factor activating transcription factor 4 (ATF4), that is preferentially translated on activation of PERK, induces the expression of C/EBP-homologous protein (CHOP/GADD153), a transcription factor with proapoptotic functions [22]. In accordance with these previous findings, the mRNA level of CHOP increased gradually after HCMV infection in NSPC/iPSCs (Figure 4H). These results suggest that UPR is involved in the activation of caspase cascade leading to apoptosis in HCMV-infected NSPC/iPSCs.

Discussion

Important findings in this study are as follows: i) NSPC/iPSCs derived from MRC-iPS-25 cells were susceptible to HCMV infection and allow the expression of viral gene products of both early and late functions and production of infectious virions. In contrast, MRC-iPS-25 cells before induction of differentiation was either resistant to HCMV or did not support the expression of HCMV immediate-early genes; ii) the HCMV-infected NSPCs undergo apoptosis; and iii) the mechanism of the apoptosis included cytochrome c release from mitochondria to cytosol and activation of UPR-related signaling pathways.

Neuropathogenesis of HCMV infection has been studied mainly with neural cells isolated from human brain. These studies demonstrated that HCMV can infect human neural precursor cells (NPCs) isolated from fetal brains and interfere with their differentiation. Luo et al. [23] showed that HCMV infection in primary NPCs reduced the expression of Nestin, suggesting that HCMV affects the differentiation potential of NPCs. Similar results were also obtained from experiments with mouse NSCs infected with MCMV [10,13,24]. Those previous findings obtained from experiments with primary cultures of brain-derived neural cells were thus mostly reproduced in our experiments using NSPC/iPSCs. In addition, similar to the results of Odeberg et al. [8] that used NPCs derived from human brain, we also demonstrated that HCMV infection induced apoptosis in NSPC/iPSCs obtained from iPSCs. It is thus supposed that neural cells differentiated from iPSCs are a useful

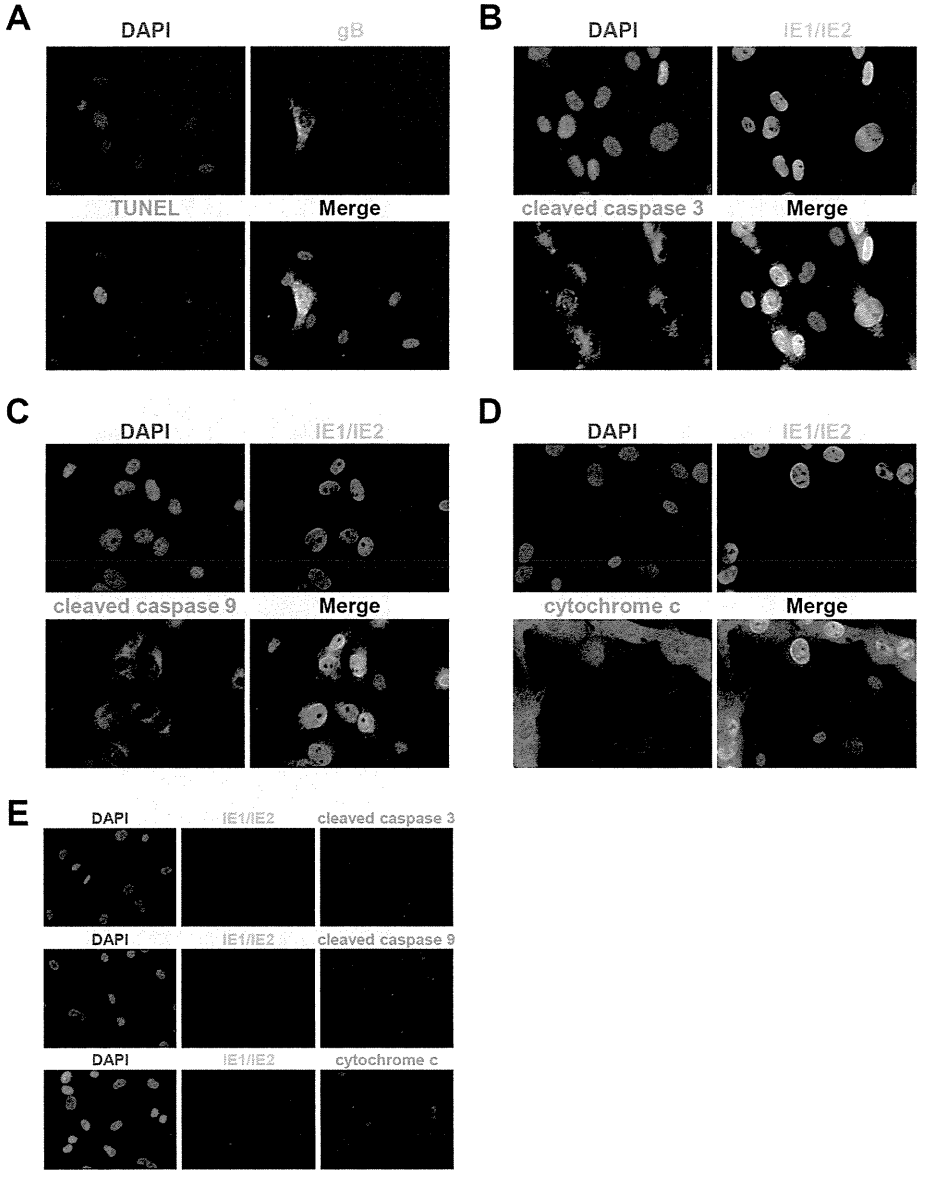

Figure 3 HCMV-induced apoptosis of NSPC/iPSCs. (A) Towne-infected NSPC/iPSCs at 6 dpi were subjected to TUNEL assay followed by immunofluorescence test with an anti-gB antibody. TUNEL-positive nuclei were stained in red. The anti-gB antibody was detected with Alexa Fluor 488-conjugated goat anti-mouse IgG antibody (green). Nuclei were stained with DAPI. **(B-D)** Towne-infected NSPC/iPSCs at 3 dpi were subjected to immunofluorescence test with anti-IE1/IE2 antibody in combination with anti-cleaved caspase 3 **(B)**, anti-cleaved caspase 9 **(C)**, or anti-cytochrome c **(D)** antibody. Alexa Fluor 488-conjugated goat anti-mouse IgG (green) or Alexa Fluor 594-conjugated goat anti-rabbit IgG antibody (red) was used as a secondary antibody. Nuclei were stained with DAPI. **(E)** Mock-infected NSPC/iPSCs were subjected to immunofluorescence test with anti-IE1/IE2 antibody in combination with anti-cleaved caspase 3 (upper panel), anti-cleaved caspase 9 (middle panel), or anti-cytochrome c (lower panel) antibody. Nuclei were stained with DAPI. Representative results from two independent experiments are shown.

model to investigate neural pathogenesis of HCMV. In the human brain, NSCs are predominantly found in the subventricular region where CMV infections preferentially occur [25,26]. Analysis on the effects of HCMV infection on NSPCs can be therefore particularly relevant.

In the regulation of cellular apoptotic responses, mitochondrial dysfunction and ER stress are involved in the activation of the initiator caspase caspase-9 that functions as a trigger of cascade protease reactions leading to cell death. The finding of cytochrome c release from mitochondria to cytoplasm in HCMV-infected NSPC/iPSCs indicates that mitochondrial dysfunction is involved in the activation of caspase-9 in these cells. In addition, the demonstration of phosphorylated forms of proteins involved in UPR, including PERK, JNK, IRE1α, eIF2α, as well as that of unconventional splicing of

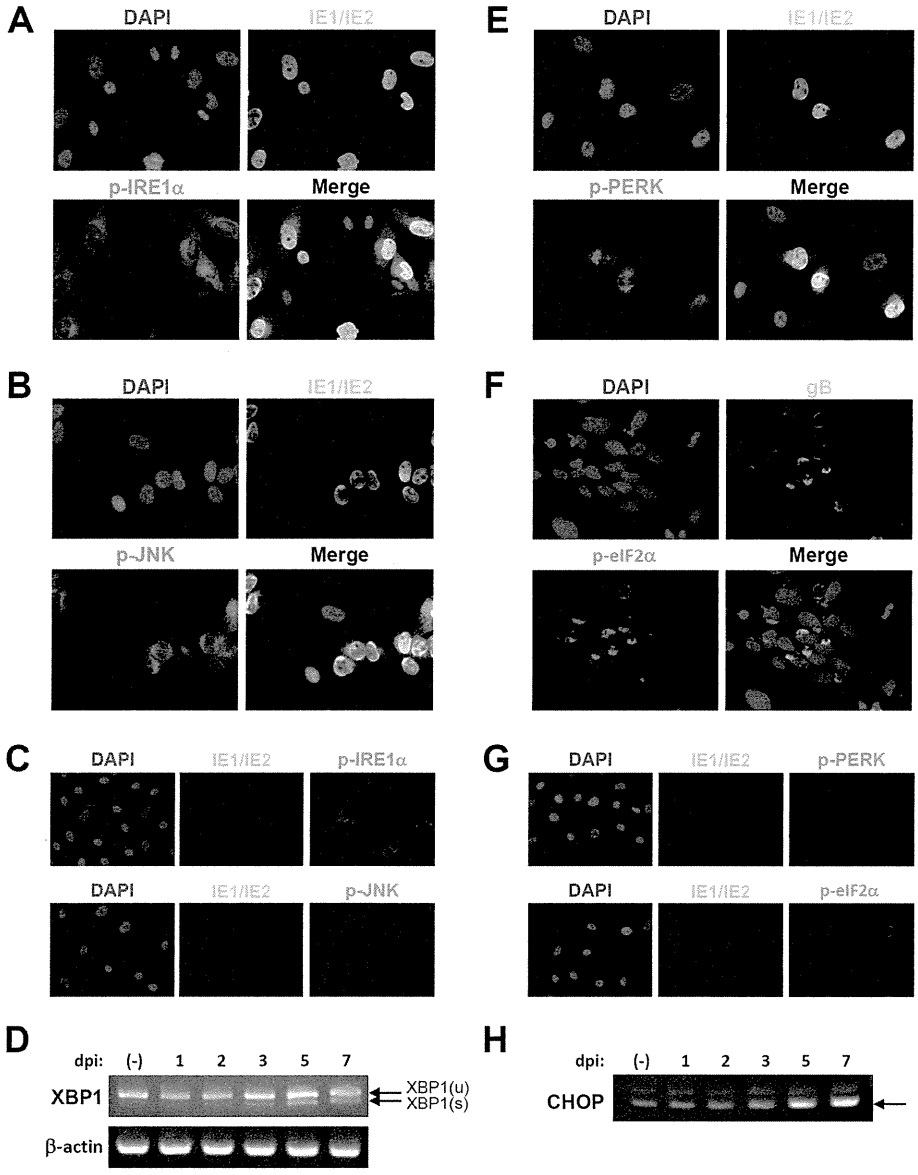

Figure 4 HCMV-induced UPR in NSPC/iPSCs. (A and B) Towne-infected NSPC/iPSCs at 3 dpi were subjected to immunofluorescence test with anti-IE1/IE2 antibody in combination with anti-phosphorylated IRE1α **(A)** or anti-phosphorylated JNK **(B)** antibody. Nuclei were stained with DAPI. **(C)** Mock-infected NSPC/iPSCs were subjected to immunofluorescence test with anti-IE1/IE2 antibody in combination with anti-phosphorylated IRE1α (upper panel) or anti-phosphorylated JNK (lower panel) antibody. Nuclei were stained with DAPI. **(D)** Detection of XBP1 (u, unspliced) and XBP1 (s, spliced) mRNAs in HCMV-infected NSPC/iPSCs. Total RNAs isolated from NSPC/iPSCs harvested before (–) HCMV infection or at 1, 2, 3, 5, and 7 dpi with HCMV Towne strain were subjected to RT-PCR assays. Amplified DNA fragments were separated in a 2% agarose gel and then photographed. Beta-actin gene expression was assayed for the control. **(E and F)** Towne-infected NSPC/iPSCs at 3 dpi were subjected to immunofluorescence test with anti-IE1/IE2 antibody in combination with anti-phosphorylated PERK **(E)** or anti-gB antibody in combination with anti-phosphorylated eIF2α **(F)** antibody. **(G)** Mock-infected NSPC/iPSCs were subjected to immunofluorescence test with anti-IE1/IE2 antibody in combination with anti-phosphorylated PERK (upper panel) or anti-phosphorylated eIF2α (lower panel) antibody. Nuclei were stained with DAPI. **(H)** Expression of CHOP mRNA in HCMV-infected NSPC/iPSCs. Total RNAs isolated from NSPC/iPSCs harvested before (–) HCMV infection or at 1, 2, 3, 5, and 7 dpi with HCMV Towne strain were subjected to RT-PCR assays. Representative results from three independent experiments are shown.

XBP1 mRNA and up-regulation of CHOP, indicate that ER stress also plays a role in HCMV-induced apoptosis of NSPC/iPSCs. These results are in accordance with the work reported by Isler et al. [27] who demonstrated that HCMV-induced UPR in human foreskin fibroblasts. HCMV is known to encode anti-apoptotic proteins such as viral inhibitor of caspase-8-induced apoptosis (vICA) encoded by UL36 [28], and pUL38 which protects against ER stress-induced cell death by modulating the UPR pathway [29]. Our RT-PCR analysis demonstrated

that such viral anti-apoptotic genes were expressed at transcription level in NSPC/iPSCs following HCMV infection (Figure 2B). Although these viral anti-apoptotic proteins did not block apoptosis of NSPC/iPSCs, they might have contributed for efficient viral replication by delaying apoptosis.

iPSCs are expected to be an innovative tool for not only regenerative medicine but also for the elucidation of pathogenesis of various diseases. Recent studies have shown that human iPSCs can be used also for modeling viral infection. Hepatocyte-like cells derived from human iPSCs were shown to be susceptible to hepatitis virus C infection and supported its replication [30,31]. Sensory neurons derived from human iPSCs were reported to be susceptible to infection with both varicella-zoster virus and herpes simplex virus [32]. While the present work was in progress, D'Aiuto and others reported on the preparation of an iPSC-derived model of HCMV infection in neural precursor cells [33]. Whereas our data described in the present study is largely consistent with their results, we further analyzed the mechanisms of apoptosis induction and elucidated the involvement of mitochondrial dysfunction and ER stress.

In conclusion, human NSPCs derived from iPSCs can be a useful model to study HCMV neuropathogenesis associated with congenital HCMV infection. They can be particularly valuable in analyzing the mechanisms of HCMV-induced apoptosis in neural cells.

Abbreviations

HCMV: Human cytomegalovirus; iPSC: Induced pluripotent stem cell; ESC: Embryonic stem cell; NSPC: Neural stem/progenitor cell; TUNEL: Terminal deoxynucleotidyl transferase-mediated dUTP nick-end labeling; UPR: Unfolded protein response; ER: Endoplasmic reticulum; PERK: PKR-like eukaryotic initiation factor 2a kinase; JNK: c-Jun NH2-terminal kinase; IRE1: Inositol-requiring enzyme 1; eIF2α: Alpha subunit of eukaryotic initiation factor 2; CHOP: C/EBP-homologous protein; XBP1: X-box binding protein 1; IFA: Indirect immunofluorescence assay; Dpi: Days post-infection; MAP2: Microtubule-associated protein 2; GFAP: Glial fibrillary acidic protein; OSP: Oligodendrocyte-specific protein; ATF4: Activating transcription factor 4; MOI: Multiplicity of infection.

Competing interests

The authors declare that they have no competing interests.

Authors' contributions

HN, HL, KM, and HA performed the experimental studies, and KI helped to analyze the data. KM, MT, HA, YM, HO, NK, and AU participated in the characterization of iPSCs and their derivatives. HN, HL, and SF wrote the manuscript. NI revised the manuscript. All authors read and approved the final manuscript.

Acknowledgments

We especially thank M. Katata for excellent technical assistance. This work was partly supported by Grants-in-Aid for Scientific Research from the Ministry of Education, Culture, Sports, Science and Technology of Japan (24591616), the Ministry of Health, Labour and Welfare of Japan (H23-Jisedai-Ippan-001), and the Grants of National Center for Child Health and Development (22A-9 and 24–17).

Author details

[1]Department of Infectious Diseases, National Research Institute for Child Health and Development, 2-10-1 Okura, Setagaya-ku, Tokyo 157-8535, Japan. [2]Department of Reproductive Biology, Center for Regenerative Medicine, National Research Institute for Child Health and Development, 2-10-1 Okura, Setagaya-ku, Tokyo 157-8535, Japan. [3]Department of Pediatric Hematology and Oncology Research, National Research Institute for Child Health and Development, 2-10-1 Okura, Setagaya-ku, Tokyo 157-8535, Japan. [4]Department of Virology I, National Institute of Infectious Diseases, 1-23-1 Toyama, Shinjuku-ku, Tokyo 162-8640, Japan.

Received: 17 April 2013 Accepted: 15 October 2013
Published: 21 October 2013

References

1. Cheeran MC, Lokensgard JR, Schleiss MR: **Neuropathogenesis of congenital cytomegalovirus infection: disease mechanisms and prospects for intervention.** *Clin Microbiol Rev* 2009, **22**(1):99–126. Table of Contents.
2. Revello MG, Gerna G: **Diagnosis and management of human cytomegalovirus infection in the mother, fetus, and newborn infant.** *Clin Microbiol Rev* 2002, **15**(4):680–715.
3. Koyano S, Inoue N, Oka A, Moriuchi H, Asano K, Ito Y, Yamada H, Yoshikawa T, Suzutani T: **Screening for congenital cytomegalovirus infection using newborn urine samples collected on filter paper: feasibility and outcomes from a multicentre study.** *BMJ Open* 2011, **1**(1):e000118.
4. Cinatl J Jr, Vogel JU, Cinatl J, Weber B, Rabenau H, Novak M, Kornhuber B, Doerr HW: **Long-term productive human cytomegalovirus infection of a human neuroblastoma cell line.** *Int J Cancer* 1996, **65**(1):90–96.
5. Cinatl J Jr, Cinatl J, Vogel JU, Kotchetkov R, Driever PH, Kabickova H, Kornhuber B, Schwabe D, Doerr HW: **Persistent human cytomegalovirus infection induces drug resistance and alteration of programmed cell death in human neuroblastoma cells.** *Cancer Res* 1998, **58**(2):367–372.
6. Luo MH, Fortunato EA: **Long-term infection and shedding of human cytomegalovirus in T98G glioblastoma cells.** *J Virol* 2007, **81**(19):10424–10436.
7. Ogura T, Tanaka J, Kamiya S, Sato H, Ogura H, Hatano M: **Human cytomegalovirus persistent infection in a human central nervous system cell line: production of a variant virus with different growth characteristics.** *J Gen Virol* 1986, **67**(Pt 12):2605–2616.
8. Odeberg J, Wolmer N, Falci S, Westgren M, Seiger A, Soderberg-Naucler C: **Human cytomegalovirus inhibits neuronal differentiation and induces apoptosis in human neural precursor cells.** *J Virol* 2006, **80**(18):8929–8939.
9. Odeberg J, Wolmer N, Falci S, Westgren M, Sundtrom E, Seiger A, Soderberg-Naucler C: **Late human cytomegalovirus (HCMV) proteins inhibit differentiation of human neural precursor cells into astrocytes.** *J Neurosci Res* 2007, **85**(3):583–593.
10. Cheeran MC, Jiang Z, Hu S, Ni HT, Palmquist JM, Lokensgard JR: **Cytomegalovirus infection and interferon-gamma modulate major histocompatibility complex class I expression on neural stem cells.** *J Neurovirol* 2008, **14**(5):437–447.
11. Matsukage S, Kosugi I, Kawasaski H, Miura K, Kitani H, Tsutsui Y: **Mouse embryonic stem cells are not susceptible to cytomegalovirus but acquire susceptibility during differentiation.** *Birth Defects Res A Clin Mol Teratol* 2006, **76**(2):115–125.
12. Li RY, Tsutsui Y: **Growth retardation and microcephaly induced in mice by placental infection with murine cytomegalovirus.** *Teratology* 2000, **62**(2):79–85.
13. Kosugi I, Shinmura Y, Kawasaki H, Arai Y, Li RY, Baba S, Tsutsui Y: **Cytomegalovirus infection of the central nervous system stem cells from mouse embryo: a model for developmental brain disorders induced by cytomegalovirus.** *Lab Invest* 2000, **80**(9):1373–1383.
14. Nishino K, Toyoda M, Yamazaki-Inoue M, Fukawatase Y, Chikazawa E, Sakaguchi H, Akutsu H, Umezawa A: **DNA methylation dynamics in human induced pluripotent stem cells over time.** *PLoS Genet* 2011, **7**(5):e1002085.
15. Makino H, Toyoda M, Matsumoto K, Saito H, Nishino K, Fukawatase Y, Machida M, Akutsu H, Uyama T, Miyagawa Y, *et al*: **Mesenchymal to embryonic incomplete transition of human cells by chimeric OCT4/3 (POU5F1) with physiological co-activator EWS.** *Exp Cell Res* 2009, **315**(16):2727–2740.
16. Chambers SM, Fasano CA, Papapetrou EP, Tomishima M, Sadelain M, Studer L: **Highly efficient neural conversion of human ES and iPS cells by dual inhibition of SMAD signaling.** *Nat Biotechnol* 2009, **27**(3):275–280.

17. Nakamura H, Lu M, Gwack Y, Souvlis J, Zeichner SL, Jung JU: **Global changes in Kaposi's sarcoma-associated virus gene expression patterns following expression of a tetracycline-inducible Rta transactivator.** *J Virol* 2003, **77**(7):4205–4220.
18. White EA, Clark CL, Sanchez V, Spector DH: **Small internal deletions in the human cytomegalovirus IE2 gene result in nonviable recombinant viruses with differential defects in viral gene expression.** *J Virol* 2004, **78**(4):1817–1830.
19. Pevny LH, Sockanathan S, Placzek M, Lovell-Badge R: **A role for SOX1 in neural determination.** *Development* 1998, **125**(10):1967–1978.
20. Calfon M, Zeng H, Urano F, Till JH, Hubbard SR, Harding HP, Clark SG, Ron D: **IRE1 couples endoplasmic reticulum load to secretory capacity by processing the XBP-1 mRNA.** *Nature* 2002, **415**(6867):92–96.
21. Sidrauski C, Walter P: **The transmembrane kinase Ire1p is a site-specific endonuclease that initiates mRNA splicing in the unfolded protein response.** *Cell* 1997, **90**(6):1031–1039.
22. Scheuner D, Song B, McEwen E, Liu C, Laybutt R, Gillespie P, Saunders T, Bonner-Weir S, Kaufman RJ: **Translational control is required for the unfolded protein response and in vivo glucose homeostasis.** *Mol Cell* 2001, **7**(6):1165–1176.
23. Luo MH, Hannemann H, Kulkarni AS, Schwartz PH, O'Dowd JM, Fortunato EA: **Human cytomegalovirus infection causes premature and abnormal differentiation of human neural progenitor cells.** *J Virol* 2010, **84**(7):3528–3541.
24. Mutnal MB, Cheeran MC, Hu S, Lokensgard JR: **Murine cytomegalovirus infection of neural stem cells alters neurogenesis in the developing brain.** *PLoS One* 2011, **6**(1):e16211.
25. Grassi MP, Clerici F, Perin C, D'Arminio Monforte A, Vago L, Borella M, Boldorini R, Mangoni A: **Microglial nodular encephalitis and ventriculoencephalitis due to cytomegalovirus infection in patients with AIDS: two distinct clinical patterns.** *Clin Infect Dis* 1998, **27**(3):504–508.
26. Perlman JM, Argyle C: **Lethal cytomegalovirus infection in preterm infants: clinical, radiological, and neuropathological findings.** *Ann Neurol* 1992, **31**(1):64–68.
27. Isler JA, Skalet AH, Alwine JC: **Human cytomegalovirus infection activates and regulates the unfolded protein response.** *J Virol* 2005, **79**(11):6890–6899.
28. Skaletskaya A, Bartle LM, Chittenden T, McCormick AL, Mocarski ES, Goldmacher VS: **A cytomegalovirus-encoded inhibitor of apoptosis that suppresses caspase-8 activation.** *Proc Natl Acad Sci U S A* 2001, **98**(14):7829–7834.
29. Terhune S, Torigoi E, Moorman N, Silva M, Qian Z, Shenk T, Yu D: **Human cytomegalovirus UL38 protein blocks apoptosis.** *J Virol* 2007, **81**(7):3109–3123.
30. Schwartz RE, Trehan K, Andrus L, Sheahan TP, Ploss A, Duncan SA, Rice CM, Bhatia SN: **Modeling hepatitis C virus infection using human induced pluripotent stem cells.** *Proc Natl Acad Sci U S A* 2012, **109**(7):2544–2548.
31. Wu X, Robotham JM, Lee E, Dalton S, Kneteman NM, Gilbert DM, Tang H: **Productive hepatitis C virus infection of stem cell-derived hepatocytes reveals a critical transition to viral permissiveness during differentiation.** *PLoS Pathog* 2012, **8**(4):e1002617.
32. Lee KS, Zhou W, Scott-McKean JJ, Emmerling KL, Cai GY, Krah DL, Costa AC, Freed CR, Levin MJ: **Human sensory neurons derived from induced pluripotent stem cells support varicella-zoster virus infection.** *PLoS One* 2012, **7**(12):e53010.
33. D'Aiuto L, Di Maio R, Heath B, Raimondi G, Milosevic J, Watson AM, Bamne M, Parks WT, Yang L, Lin B, *et al*: **Human induced pluripotent stem cell-derived models to investigate human cytomegalovirus infection in neural cells.** *PLoS One* 2012, **7**(11):e49700.

doi:10.1186/2042-4280-4-2
Cite this article as: Nakamura *et al.*: Human cytomegalovirus induces apoptosis in neural stem/progenitor cells derived from induced pluripotent stem cells by generating mitochondrial dysfunction and endoplasmic reticulum stress. *Herpesviridae* 2013 4:2.

International Journal of Infectious Diseases 17 (2013) e1092–e1097

Contents lists available at SciVerse ScienceDirect

International Journal of Infectious Diseases

journal homepage: www.elsevier.com/locate/ijid

Perspective

Polymorphisms in TLR-2 are associated with congenital cytomegalovirus (CMV) infection but not with congenital CMV disease

Rumi Taniguchi [a,b], Shin Koyano [c], Tatsuo Suzutani [d], Keiji Goishi [b], Yushi Ito [e], Ichiro Morioka [f], Akira Oka [b,g], Hiroyuki Nakamura [h], Hideto Yamada [i], Takashi Igarashi [b], Naoki Inoue [a,*]

[a] Department of Virology I, National Institute of Infectious Diseases, 1-23-1 Toyama Shinjuku-ku, Tokyo 162-8640, Japan
[b] Department of Pediatrics, The University of Tokyo, Tokyo, Japan
[c] Department of Pediatrics, Asahikawa Medical University, Asahikawa, Japan
[d] Department of Microbiology, Fukushima Medical University, Fukushima, Japan
[e] Department of Maternal and Perinatal Services, National Center for Child Health and Development, Tokyo, Japan
[f] Department of Pediatrics, Kobe University, Kobe, Japan
[g] Department of Pediatrics, Kyorin University, Tokyo, Japan
[h] Department of Infectious Diseases, National Center for Child Health and Development, Tokyo, Japan
[i] Department of Obstetrics and Gynecology, Kobe University, Kobe, Japan

ARTICLE INFO

Article history:
Received 15 April 2013
Received in revised form 4 June 2013
Accepted 6 June 2013

Corresponding Editor: Eskild Petersen, Aarhus, Denmark

Keywords:
Cytomegalovirus
Congenital infection
Toll-like receptors
Polymorphisms

SUMMARY

Background: Cytomegalovirus (CMV) is the most common cause of congenital virus infection. However, the risk factors for infection in utero and for progression to a severe clinical outcome remain uncertain. Recent studies have identified associations of specific single nucleotide polymorphisms (SNPs) in Toll-like receptor (TLR) genes with susceptibility to infections of some viruses and with their clinical outcome.

Methods: Genetic polymorphisms in the TLR-2, TLR-4, and TLR-9 genes were analyzed in 87 children with congenital CMV infections by the TaqMan allelic discrimination assay. The frequencies of genotypes in the general Japanese population were obtained from the National Center for Biotechnology Information (NCBI) databases. Associations between the analyzed SNPs and congenital CMV infection or disease were evaluated.

Results: The CC genotype at SNP rs3804100 in the TLR-2 gene was significantly associated with congenital CMV infection but not with congenital CMV disease. Furthermore, the AG genotype at SNP rs1898830 in the TLR-2 gene tended to be identified less frequently in children with congenital CMV infection. There were no statistically significant associations between SNPs in the TLR-4 and TLR-9 genes and congenital CMV infection or disease.

Conclusion: TLR-2 polymorphisms may have some association with congenital CMV infection, although the mechanism underlying this effect remains to be clarified.

1. Introduction

Human cytomegalovirus (CMV) is a leading cause of congenital virus infections in developed countries, such as the USA, where rubella has been eliminated and antiviral treatment is available for HIV.[1] The risk of transmission of CMV to the fetus due to primary maternal infection during pregnancy ranges from 14% to 52%.[2,3] As many as 10–15% of infants with congenital CMV infection exhibit severe, classic 'cytomegalic inclusion disease', characterized by intrauterine growth retardation (IUGR), jaundice, hepatosplenomegaly, and thrombocytopenia, while the remaining 85–90% are asymptomatic at birth.[3] In addition, CMV causes late-onset neurological sequelae, such as sensorineural hearing loss (SNHL) and developmental delay. In our congenital CMV screening program, we analyzed 21 272 newborns and identified 66 cases with congenital CMV infection (0.31%).[4] Thirty percent of the cases had typical clinical manifestations and/or showed abnormalities in brain images at birth.

The potential risk factors for congenital CMV infection or disease may include both viral and host factors. For example, viral loads in the blood but not viral genotypes may influence clinical outcomes.[5–7] Host factors may include CMV-IgG avidity levels in pregnant women, and cytotoxic T lymphocyte responses and innate immunity in fetuses.[8–10] There have been few studies on the

* Corresponding author. Tel.: +81 3 4582 2663; fax: +81 3 5285 1180.
E-mail address: ninoue@nih.go.jp (N. Inoue).

1201-9712/$36.00 – see front matter © 2013 International Society for Infectious Diseases. Published by Elsevier Ltd. All rights reserved.
http://dx.doi.org/10.1016/j.ijid.2013.06.004

association between innate immunity and congenital CMV infection.[11] As fetuses and newborns have poor acquired immunity, the innate immune system seems to have an important role.[9,12]

A growing accumulation of data has indicated that specific single nucleotide polymorphisms (SNPs) in several Toll-like receptor (TLR) genes have some association with an altered susceptibility to, or clinical outcome of, infectious diseases.[13] SNPs in the TLR genes are associated with CMV disease in transplant recipients.[14–16] It is considered that CMV glycoproteins B and H stimulate the TLR-2 signal pathway, resulting in nuclear factor kappa B (NF-κB) activation and the production of inflammatory cytokines.[17,18] Although the direct involvement of TLR-4 in CMV recognition has not been reported, dendritic cells stimulated by TLR ligands enhance CMV-specific CD4+ and CD8+ T cell responses.[19] TLR-9 is critical to the process of CMV sensing to assure rapid antiviral responses.[20,21] Here we examined whether SNPs in the TLR-2, TLR-4, and TLR-9 genes have any predictive values for congenital CMV infection and for progression into CMV disease.

2. Methods

2.1. Human subjects

This study was approved by the ethics committee on human subjects of each participating institute. We obtained informed consent from the parents of enrolled participants. In this study, the following 87 cases with congenital CMV infection (group B, Figure 1) were analyzed. (1) Forty-eight cases (nine symptomatic and 39 asymptomatic at birth, and four developed a late-onset disease) identified in our prospective study: we previously conducted a urine filter-based screening program for congenital CMV infection and identified 66 cases from 21 272 babies born at 25 diverse study sites in six geographically separate areas of Japan, without any selection bias.[4] Blood specimens of 48 out of the 66 cases were used in this study based merely on their availability. (2) Twenty-one cases who visited one of the study sites because of developmental delay or SNHL and were diagnosed with congenital CMV infection by retrospective assay using dried umbilical cord specimens;[22] 15 of them were asymptomatic at birth. (3) Eighteen cases who were suspected of congenital CMV infection before or at birth and were conclusively diagnosed both by PCR detection and by virus isolation of CMV in urine within 3 weeks after birth;[5,23] three of them were asymptomatic at birth and two developed a late-onset disease(s).

Instead of recruiting healthy infants as a control group, we used the information from the database for the general Japanese population as described below.

2.2. Clinical evaluation

Clinical information for all participants, including clinical manifestations and results of audiological tests and brain imaging, were extracted from their medical records. All infants diagnosed at birth were followed up for 3.18 ± 1.14 years (range 1.5–5.8 years). There was no statistical difference in the follow-up periods of groups E and F. Mental and physical development was closely monitored at outpatient clinics. Audiological tests were performed using auditory brainstem responses and/or auditory steady-state responses, and brain imaging was done by computed tomography and/or magnetic resonance imaging. All participants underwent audiological tests and brain imaging.

We defined 'symptomatic cases at birth' (group D) as any infant with one or more clinically significant manifestation at birth, including microcephaly, chorioretinitis, SNHL, and a combination of petechiae, hepatosplenomegaly, and jaundice. IUGR alone and manifestations that are not pathognomonic for congenital CMV infection, such as arrhythmia and ventricular septal defect (VSD), were excluded from the category. Cases 'symptomatic at birth and/or developed permanent sequelae' (group F) included (1) 'symptomatic cases at birth' (group D), (2) any infants with CMV-associated major abnormalities in their brain imaging at birth or later on, such as intracranial calcifications, ventriculomegaly, and white matter disease, and/or (3) any infants with late-onset symptoms, including SNHL, chorioretinitis, and developmental delay (group H). 'Asymptomatic cases' (group E) were defined as those who were not categorized into group D in their follow-up periods. In addition to cases without any manifestations, four cases with IUGR, one with VSD, and two with arrhythmia were classified into group E.

2.3. Analysis of SNPs

Genomic DNA was extracted from peripheral blood mononuclear cells or from dried umbilical cord specimens, using a commercial kit. Integrity and quantity of the extracted DNA specimens were evaluated by qPCR using the human albumin gene as a target.[22]

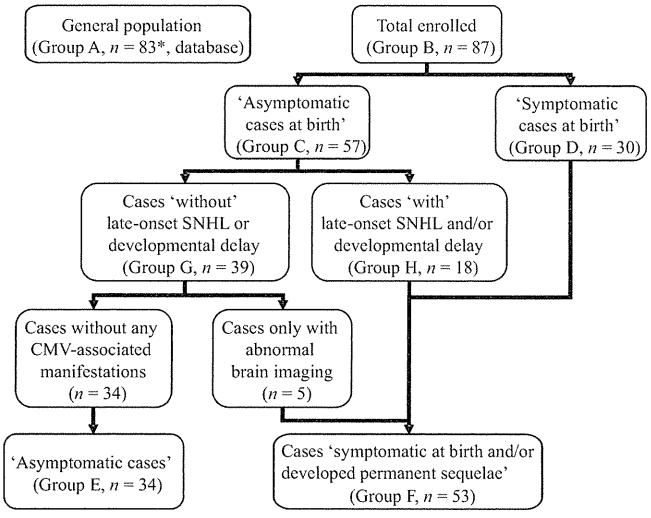

Figure 1. Grouping of the cases in the study cohort. To analyze the associations between target gene SNPs and congenital CMV infection or disease, participants were divided into the groups as shown. The group codes are used in Tables 1 and 2. *Samples of rs3804100 in TLR-2 obtained from the database. Number of samples of other SNPs shown in the text. (SNHL, sensorineural hearing loss.)